

# Prediction of Fractures in Men Using Bone Microarchitectural Parameters Assessed by High-Resolution Peripheral Quantitative Computed Tomography—The Prospective STRAMBO Study

Pawel Szulc, Stéphanie Boutroy, and Roland Chapurlat

INSERM UMR 1033, University of Lyon, Hospices Civils de Lyon, Lyon, France

## ABSTRACT

Areal bone mineral density (aBMD) poorly identifies men at high fracture risk. Our aim was to assess prediction of fractures in men by bone microarchitectural measures. At baseline, 825 men aged 60 to 87 years had the assessment of bone microarchitecture at distal radius and distal tibia by high-resolution peripheral QCT (HR-pQCT; XtremeCT-I, Scanco Medical, Brüttisellen, Switzerland). Bone strength was estimated by micro-finite element analysis. During the prospective 8-year follow-up, 105 men sustained fractures (59 vertebral fractures in 49 men and 70 nonvertebral fractures in 68 men). After adjustment for age, body mass index (BMI), prior falls, and fractures, most HR-pQCT measures at both skeletal sites predicted fractures. After further adjustment for aBMD, low distal radius trabecular number (Tb.N) was most strongly associated with higher fracture risk (hazard ratio [HR] = 1.63 per SD, 95% confidence interval [CI] 1.31–2.03,  $p < 0.001$ ). In similar models, low Tb.N was associated with higher risk of major osteoporotic fracture (HR = 1.80 per SD,  $p < 0.001$ ), vertebral fracture (HR = 1.78 per SD,  $p < 0.01$ ) and nonvertebral fracture (HR = 1.46 per SD,  $p < 0.01$ ). In comparison with the reference model (age, BMI, falls, fractures, aBMD), the adjustment for distal radius Tb.N increased the estimated fracture probability in men who sustained fractures versus those who did not have ones (difference = 4.1%, 95% CI 1.9–6.3%,  $p < 0.001$ ). However, the adjustment for distal radius Tb.N did not increase the area under the curve (AUC,  $p = 0.37$ ). Similar results were found for distal radius trabecular separation (Tb.Sp) and connectivity density (Conn. D). They were predictive of all fracture types and increased the estimated fracture risk, but not AUC, in men who had incident fractures. Thus, poor distal radius trabecular microarchitecture is predictive of fracture after adjustment for age, BMI, falls, fractures, and aBMD. Although distal radius Tb.N, Conn. D, and Tb.Sp improve the discrimination between men who will or who will not have fracture, they do not provide clinically relevant improvement of fracture prediction in older men. © 2018 American Society for Bone and Mineral Research.

**KEY WORDS:** FRACTURE RISK ASSESSMENT; FRACTURE; HIGH-RESOLUTION PERIPHERAL QCT; COHORT STUDY; MEN

## Introduction

Osteoporosis in older men is a major public health problem. Increasing life expectancy results in a greater number of older men at high risk of fracture.<sup>(1)</sup> Fractures are associated with higher morbidity and mortality in men than in women.<sup>(2)</sup> However, areal bone mineral density (aBMD) measured by dual-energy X-ray absorptiometry (DXA) poorly identifies men at high risk of fracture.<sup>(3,4)</sup> Bone turnover markers, sex steroids, ultrasounds, and quantitative computed tomography (QCT) of proximal femur do not improve fracture prediction in older men compared with aBMD.<sup>(5–8)</sup>

FRAX accounts for additional risk factors (lifestyle, parental history of hip fracture, etc.) in the assessment of the fracture risk.<sup>(9)</sup> Further adjustment for trabecular bone score (TBS) adds information on bone structure derived from lumbar spine DXA scans.<sup>(10)</sup> However, in the fracture prediction in older men,

superiority of the TBS-corrected FRAX versus the classical model (age, aBMD, prior falls, and fractures) is modest.<sup>(11–14)</sup> The studies on the improvement of fracture prediction by TBS yielded inconsistent results in men.<sup>(11,13,15)</sup>

Therefore, it is urgent to look for other diagnostic methods to improve fracture prediction in older men. Bone microarchitecture is a determinant of bone strength regardless of bone mass.<sup>(16)</sup> Cross-sectional studies show that poor bone microarchitecture assessed by high-resolution peripheral QCT (HR-pQCT) is associated with higher odds of fracture in postmenopausal women and older men.<sup>(17–20)</sup> Some microarchitectural variables remained significant after adjustment for aBMD.<sup>(17–20)</sup> Finally, in postmenopausal women, bone microarchitectural and biomechanical measures assessed by HR-pQCT and micro-finite element analysis ( $\mu$ FEA) were predictive of fragility fracture after adjustment for aBMD.<sup>(21)</sup>

Thus, our primary aim was to study whether bone microarchitectural and  $\mu$ FEA measures were associated with higher

Received in original form December 14, 2017; revised form April 9, 2018; accepted April 15, 2018. Accepted manuscript online April 25, 2018.

Address correspondence to: Pawel Szulc, MD, PhD, INSERM UMR 1033, Hôpital Edouard Herriot, Pavillon F, Place d'Arsonval, 69437 Lyon, France. E-mail: pawel.szulc@inserm.fr

Journal of Bone and Mineral Research, Vol. 33, No. xx, Month 2018, pp 1–10

DOI: 10.1002/jbmr.3451

© 2018 American Society for Bone and Mineral Research

risk of fracture in older men. If so, our secondary aim was to establish which measures, used as continuous variable or categorized according to its most discriminating threshold, improve fracture prediction compared with other indicators of fracture risk.

## Subjects and Methods

### Cohort

The STRAMBO study is a single-center prospective cohort study of the skeletal fragility and its determinants in men.<sup>(22)</sup> It was carried out as collaboration between INSERM (National Institute of Health and Medical Research) and MTRL (Mutuelle des Travailleurs de la Région Lyonnaise). MTRL is a complementary health insurance company, open to all citizens. Its insured are representative of the French population in terms of age groups and of the proportion between white-collar and blue-collar workers. The study obtained authorization from the local ethics committee and was performed in agreement with the Helsinki Declaration of 1975 and 1983. Participants were recruited in 2006 to 2008 from the MTRL lists in Lyon. Letters inviting participation were sent to a randomly selected sample of men aged 20 to 85 years living in greater Lyon. Informed consent was provided by 1169 men. All men able to give informed consent, to answer interviewer-administered questionnaires, and to participate in the diagnostic tests were included. No specific exclusion criteria were used. We offered the transport to men who needed it. Men aged 60 and older ( $n = 825$ ) were followed up prospectively for 8 years. Every year they replied to a short questionnaire sent by mail and concerning incident nonvertebral fractures. After 4 and 8 years, they had a full follow-up visit.

### High-resolution peripheral quantitative computed tomography (HR-pQCT)

Microarchitecture was assessed at baseline at the non-dominant distal radius and at the right distal tibia using the Xtreme-CT-I device (Scanco Medical, Brüttisellen, Switzerland).<sup>(22)</sup> The arm or the leg was immobilized in a carbon-fiber shell. A scout view was used to set a reference line. The most distal CT slice was placed 9.5 and 22.5 mm proximal to the endplate of the radius and tibia, respectively. A 3D stack of 110 slices was acquired starting 9.5 mm from the reference line with an isotropic voxel size of 82  $\mu\text{m}$ . The volume of interest (VOI) is separated into trabecular and cortical compartments using a threshold-based algorithm. Cortical thickness (Ct.Th) was defined as the mean cortical volume divided by the bone perimeter. Cortical and trabecular density (Ct.vBMD, Tb.vBMD,  $\text{mg}/\text{cm}^3$ ) were calculated as average vBMD within each compartment. Trabecular elements were identified by mid-axis transformation method. Trabecular thickness (Tb.Th,  $\mu\text{m}$ ) and separation (Tb.Sp,  $\mu\text{m}$ ) were derived from BV/TV. Trabecular number (Tb.N,  $1/\text{mm}$ ) was calculated as the inverse of Tb.Sp. The intra-individual scatter of Tb.Sp (Tb.Sp. SD,  $\mu\text{m}$ ) reflects trabecular network heterogeneity. It is quantified as standard deviation of the distance between the mid-axes. Nonmetric trabecular connectivity density (Conn. D) was also assessed. Quality control was performed by daily scans of a phantom containing rods of HA (densities of 0–800  $\text{mg}/\text{HA}/\text{cm}^3$ ) embedded in a soft-tissue-equivalent resin (QRM, Moehrendorf, Germany). The coefficient of variation (CV) for the densities was 0.1% to 0.9%. Scans of poor quality (grade  $>3$ ) were excluded (radius 74, tibia 48).<sup>(23)</sup> In vivo CVs varied from 0.7% for Ct.vBMD to 4.4% for Tb.Th.<sup>(24)</sup>

Micro-FEA models of the radius and tibia were created from the HR-pQCT images using the IPL software v1.13 using the HR-pQCT device (Scanco Medical) as described previously.<sup>(21)</sup> A compression test was simulated in which a load in the longitudinal direction was applied at one end while the other end was fully constrained.<sup>(25–27)</sup> We set the critical strain to 3500  $\mu\text{strain}$ .<sup>(21)</sup> Micro-FEA outcomes included failure load (N) and stiffness (kN/mm).

### Incident fractures

Men self-reporting incident fractures were asked for medical records. We excluded fractures of skull, face, hand, fingers, and toes. We retained self-reported low-trauma fractures (fall from a standing position or less) confirmed by health professional (X-ray, medical report). Fractures related to high trauma were excluded. Lateral single-energy scans of the thoracic and lumbar spine (T<sub>4</sub> to L<sub>4</sub>) were obtained in the dorsal decubitus position using a Hologic Discovery-A (Hologic, Bedford, MA, USA) device equipped with rotating C-arm.<sup>(19)</sup> Scans were performed in all men at baseline and in those who returned for the follow-up visits (4 and 8 years). Incident vertebral fractures were assessed on the follow-up scans. A new incident fracture was diagnosed based on the visual analysis (endplate fracture) and/or a decrease in any of the vertebral heights by  $>15\%$  versus the previous scan. The vertebrae not correctly visible were considered nonfractured.

### Questionnaire and assessment of prevalent vertebral fractures

Men replied to an interviewer-administered questionnaire. They self-reported falls during the year preceding the recruitment without external force and current bisphosphonate therapy. Prior nonvertebral fractures self-reported at baseline were dichotomized (Y/N) and not verified. We retained low-trauma fractures except those of skull, face, hand, fingers, and toes. Prevalent vertebral fractures were assessed using a semiquantitative score on baseline lateral DXA scans.<sup>(19)</sup> Grades 2 and 3 fractures not related to a self-reported major trauma were retained. Weight and height were measured using standard equipment.

### Dual-energy X-ray absorptiometry (DXA)

Areal BMD was measured at baseline at lumbar spine, total hip, and non-dominant distal radius using a Hologic Discovery-A. Its stability was assessed by the spine phantom measured daily (CV = 0.35%). The in vivo CV was 1.1% to 1.2%. TBS was calculated on the anteroposterior spine scans as described previously.<sup>(28)</sup>

### Statistical methods

Statistical analyses were performed using the SAS 9.3 software (SAS, Cary, NC, USA). Continuous variables with Gaussian distribution are presented as mean and standard deviation, those with skewed distribution as median and interquartile (IQ) range, and categorical ones as percentage per class. Unadjusted and age-adjusted comparisons were made by the analysis of variance for continuous variables (log-transformed if necessary) and the chi-square test for categorical variables. Fracture-free survival according to HR-pQCT variables was analyzed by Cox model after checking the assumption of proportional hazards using the Schoenfeld residues. Follow-up

time was censored at the first fracture, death, last news, or 8 years after baseline, whichever came first. The link between HR-pQCT measures and fracture risk was assessed at first using an unadjusted model. Then, the model was adjusted for the variables known to be associated with the fracture risk and those that were significant in the bivariable comparisons: age, BMI (continuous), prior falls and fractures (Y/N), anti-osteoporosis treatment, HR-pQCT parameter, and arm length (radius) or height (tibia). The models were adjusted for falls to isolate fracture risk related to bone fragility and for prior fragility fractures because they are associated with poor bone microarchitecture and higher risk of subsequent fracture independent of other risk factors.<sup>(9,19)</sup> Then, it was adjusted for baseline aBMD (distal radius or total hip). Arm length, height, and anti-osteoporosis therapy were consistently nonsignificant ( $p > 0.3$ ) and not retained in the final model. Youden's index was calculated on the basis of the sensitivity and specificity values obtained using the unadjusted ROC curve analysis.<sup>(29)</sup> The improvement of fracture prediction by distal radius Tb.N, Tb.Sp, and Conn. D was assessed using the integrated discrimination improvement (IDI) algorithm and Harrell's statistics.<sup>(30)</sup> The reference model included age, BMI, prior falls, prior fractures, and aBMD.

## Results

### Descriptive analysis

Six men who dropped out after baseline did not differ from those who were followed, but they were older ( $p = 0.08$ ). The median follow-up was 8.0 years (interquartile range [IQR] 6.0–8.0). Among 819 men followed for  $\geq 1$  year, 105 sustained fragility fractures (Fig. 1). They were older and had lower hip aBMD than those who did not (Table 1). After adjustment for age, all baseline HR-pQCT measures at both sites (except Tb.Th) differed significantly between men who did or did not sustain any fracture. Similar results were found for major osteoporotic fractures.

### All fragility fractures

Median follow-up to the first fracture was 4 years (IQR 3.4–6.3). In unadjusted models, all HR-pQCT parameters were significantly associated with the fracture risk (Table 2). After adjustment for age, BMI, falls, and fractures, most HR-pQCT measures (except Tb.Th, radius Ct.vBMD, and tibia Conn. D) remained associated with higher fracture risk. After further adjustment for aBMD, distal radius Tb.vBMD, Tb.N, Tb.Sp, Tb.Sp.SD, and Conn. D remained associated significantly with higher fracture risk. The results remained similar after adjustment for total hip aBMD, eg, for Tb.N: hazard ratio [HR] = 1.54 per SD, 95% confidence interval [CI] 1.24–1.90,  $p < 0.001$ .

### Major osteoporotic fractures

Median follow-up to the major osteoporotic fracture was 4.2 years (IQR: 3.9; 7.0). In the unadjusted models, all HR-pQCT parameters were significantly associated with the risk of this fracture. After adjustment for age, BMI, falls, and fractures, distal radius HR-pQCT measures (except Ct.Th, Ct.vBMD, and Tb.Th) were associated with higher fracture risk. After further adjustment for aBMD, Tb.vBMD, Tb.N, Tb.Sp, Tb.Sp.SD, and Conn. D remained significant. The results were similar after adjustment for hip aBMD, eg, Tb.N: HR = 1.61 per SD, 95% CI 1.24–2.10,  $p < 0.001$ . Most distal tibia measures were also

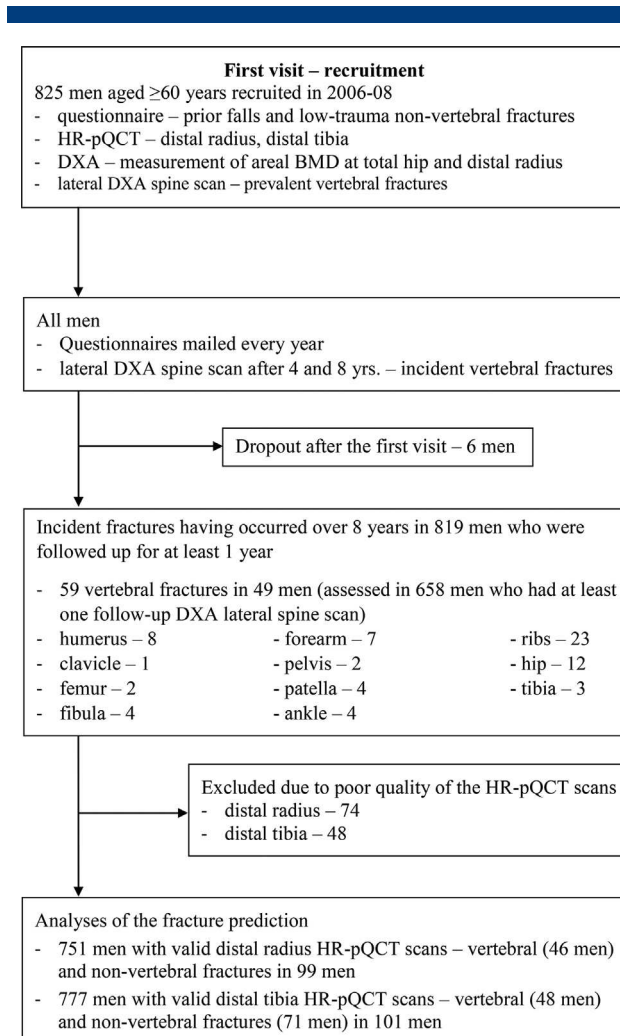


**Fig. 1.** Flowchart presenting the organization and the progress of the study.

associated with higher risk of fracture (except Tb.Th) but were no longer significant after adjustment for hip aBMD.

### Vertebral fractures

Median follow-up to diagnosis of the first vertebral fracture was 4.2 years (IQR 3.9–7.9). In the bivariable models, nearly all HR-pQCT measures predicted vertebral fractures (Table 3). Among 616 men who had follow-up DXA and valid distal radius HR-pQCT scans, 46 men had vertebral fractures. After adjustment for age, BMI, fractures, and falls, Tt.vBMD and most trabecular measures were associated with the fracture risk. After further adjustment for distal radius aBMD, Tb.vBMD, Tb.N, Tb.Sp, and Conn. D remained associated with the vertebral fracture risk. The results were similar after adjustment for total hip aBMD (Tb.N: HR = 1.52 per SD, 95% CI 1.11–2.08,  $p < 0.01$ ). Among 628 men who had valid tibia HR-pQCT and follow-up spine scans, 48 men had vertebral fractures. Low Tt.vBMD, Tb.vBMD, Tb.N, and Conn. D and high Tb.Sp and Tb.Sp.SD were associated with higher vertebral fracture risk. However, they were no longer significant after adjustment for hip aBMD.

**Table 1.** Description of Men From the STRAMBO Cohort According to the Fracture Status

	No incident fracture (n = 714)	All incident fractures (n = 105)	<i>p</i> <sup>a</sup>	Incident major osteoporotic fractures (n = 73)	<i>p</i> <sup>a</sup>
Age (years)	71.7 ± 7.2	74.8 ± 7.4	<0.001	75.1 ± 7.5	<0.001
Weight (kg)	78.5 ± 11.3	77.8 ± 11.4	0.89	76.8 ± 11.9	0.48
Height (cm)	168.4 ± 6.4	167.8 ± 6.8	0.41	166.9 ± 6.6	0.07
BMI (kg/m <sup>2</sup> )	27.7 ± 3.6	27.5 ± 3.4	0.71	27.5 ± 3.4	0.72
Arm length (cm)	26.9 ± 1.4	26.8 ± 1.2	0.84	26.7 ± 1.3	0.38
Prior fractures (n, %)	139 (19%)	29 (28%)	0.25	19 (28%)	0.13
Prior falls (n, %)	138 (19%)	31 (30%)	0.35	20 (29%)	0.63
Bisphosphonates (n, %)	18 (2.5%)	2 (1.9%)	0.72	2 (3.0%)	0.75
Lumbar spine aBMD (g/cm <sup>2</sup> )	1.051 ± 0.192	0.961 ± 0.151	<0.001	0.941 ± 0.163	<0.001
Hip aBMD (g/cm <sup>2</sup> )	0.962 ± 0.138	0.892 ± 0.129	<0.001	0.881 ± 0.128	<0.001
Femoral neck aBMD (g/cm <sup>2</sup> )	0.768 ± 0.129	0.723 ± 0.112	<0.001	0.713 ± 0.112	<0.001
Femoral neck T-score <sup>b</sup>	-0.60 ± 1.07	-1.13 ± 0.93	<0.001	-1.21 ± 0.93	<0.001
Spine TBS	1.220 ± 0.113	1.174 ± 0.108	<0.001	1.161 ± 0.117	<0.001
FRAX (major) <sup>c</sup>	3.8 (2.6; 5.6) <sup>e</sup>	5.5 (4.2; 7.3)	<0.001	5.7 (4.4; 7.6)	<0.001
FRAX (hip) <sup>d</sup>	1.0 (0.4; 2.2)	2.2 (1.1; 3.3)	<0.001	2.5 (1.6; 3.6)	<0.001
FRAX (major)	4.8 (3.3; 7.1)	6.9 (5.2; 8.7)	<0.001	7.3 (5.9; 9.1)	<0.001
TBS-adjusted FRAX (hip)	1.3 (0.6; 2.6)	2.6 (1.5; 4.0)	<0.001	2.9 (1.9; 4.1)	<0.001
TBS-adjusted Distal radius	(n = 652)	(n = 99)		(n = 69)	
Tt.vBMD (mg/cm <sup>3</sup> )	295.0 ± 64.4	264.0 ± 60.0	<0.005	260.8 ± 60.6	<0.05
Ct.vBMD (mg/cm <sup>3</sup> )	802.1 ± 70.8	774.0 ± 77.6	0.08	771.8 ± 76.4	0.30
Ct.Th (mm)	0.70 ± 0.22	0.61 ± 0.21	<0.05	0.59 ± 0.21	0.05
Tb.vBMD (mg/cm <sup>3</sup> )	174.9 ± 39.4	155.5 ± 38.3	<0.001	154.2 ± 40.5	<0.005
Tb.N (/mm)	1.87 ± 0.25	1.70 ± 0.29	<0.001	1.70 ± 0.30	<0.001
Tb.Th (µm)	78 ± 12	76 ± 13	0.81	75 ± 14	0.80
Tb.Sp (mm)	0.46 (0.41; 0.51)	0.50 (0.46; 0.57)	<0.001	0.50 (0.45; 0.58)	<0.001
Tb.Sp.SD (mm)	0.20 (0.17; 0.23)	0.22 (0.19; 0.28)	<0.001	0.22 (0.19; 0.28)	<0.001
Connectivity density	3.77 ± 0.90	3.34 ± 0.94	<0.001	3.29 ± 0.97	<0.001
Stiffness (kN/mm)	178 ± 42	166 ± 37	<0.005	165 ± 37	<0.05
Failure load (N)	4227 ± 967	3942 ± 855	<0.005	3912 ± 847	<0.05
Distal tibia	(n = 676)	(n = 101)		(n = 71)	
Tt.vBMD (mg/cm <sup>3</sup> )	290.6 ± 58.3	262.7 ± 52.7	<0.001	261.3 ± 52.1	<0.01
Ct.vBMD (mg/cm <sup>3</sup> )	834.3 ± 59.9	799.7 ± 85.3	<0.001	801.5 ± 66.6	<0.01
Ct.Th (mm)	1.19 ± 0.30	1.04 ± 0.30	<0.001	1.04 ± 0.27	<0.05
Tb.vBMD (mg/cm <sup>3</sup> )	172.9 ± 38.2	159.6 ± 36.9	<0.02	157.9 ± 39.9	<0.05
Tb.N (/mm)	1.74 ± 0.30	1.65 ± 0.32	<0.05	1.63 ± 0.32	0.05
Tb.Th (µm)	83 ± 13	81 ± 13	0.63	81 ± 13	0.74
Tb.Sp (mm)	0.49 (0.43; 0.56)	0.52 (0.46; 0.61)	<0.01	0.54 (0.48; 0.62)	<0.01
Tb.Sp.SD (mm)	0.23 (0.19; 0.27)	0.25 (0.21; 0.31)	<0.01	0.26 (0.22; 0.32)	<0.01
Connectivity density	3.36 ± 0.93	3.15 ± 0.99	<0.05	3.05 ± 0.97	<0.01
Stiffness (kN/mm)	465 ± 83	435 ± 85	<0.001	420 ± 84	<0.001
Failure load (N)	10985 ± 1887	10335 ± 1941	<0.001	9993 ± 1909	<0.001

BMI = body mass index; aBMD = areal bone mineral density; Tt.vBMD = total volumetric bone mineral density; Ct.vBMD = cortical volumetric bone mineral density; Ct.Th = cortical thickness; Tb.vBMD = trabecular volumetric bone mineral density; Tb.N = trabecular number; Tb.Th = trabecular thickness; Tb.Sp = trabecular separation; Tb.Sp.SD = standard deviation of the trabecular separation.

<sup>a</sup>Unadjusted comparisons: age, weight, height, BMI, arm length, falls, fractures, bisphosphonate use, aBMD, T-score, spine TBS, and FRAX; adjusted for age: bone microarchitectural.

<sup>b</sup>Calculated according to the reference values for the white women aged 20 to 29 years from the NHANES study.

<sup>c</sup>FRAX for major osteoporotic fractures adjusted for femoral neck aBMD.

<sup>d</sup>FRAX for hip fractures adjusted for femoral neck aBMD.

<sup>e</sup>Median (first quartile, third quartile), age-adjusted comparisons performed on the log-transformed variables.

**Table 2.** Association of the Bone Microarchitecture With the Risk of Incident Fragility Fracture and of Incident Major Osteoporotic Fractures in Older Men

	All incident fragility fractures			Major incident osteoporotic fractures		
	Unadjusted	Adjusted for age, BMI, prior falls and fractures	Additionally adjusted for aBMD <sup>f</sup>	Unadjusted	Adjusted for age, BMI, prior falls and fractures	Additionally adjusted for aBMD <sup>f</sup>
	HR per SD (95% CI) <sup>e</sup>			HR per SD (95% CI) <sup>e</sup>		
Radius	(n/N = 99/751)			(n/N = 69/751)		
Tt.vBMD	1.81 (1.45–2.27) <sup>d</sup>	1.53 (1.21–1.95) <sup>d</sup>	1.29 (0.91–1.83)	2.01 (1.51–2.67) <sup>d</sup>	1.57 (1.16–2.13) <sup>c</sup>	1.45 (0.93–2.26)
Ct.vBMD	1.49 (1.24–1.78) <sup>d</sup>	1.20 (0.97–1.49)	0.95 (0.73–1.24)	1.52 (1.22–1.91) <sup>d</sup>	1.12 (0.86–1.45)	0.86 (0.62–1.20)
Ct.Th	1.64 (1.32–2.03) <sup>d</sup>	1.32 (1.04–1.67) <sup>a</sup>	1.03 (0.76–1.40)	1.75 (1.33–2.30) <sup>d</sup>	1.28 (0.95–1.72)	1.00 (0.69–1.47)
Tb.vBMD	1.78 (1.44–2.21) <sup>d</sup>	1.55 (1.25–1.93) <sup>d</sup>	1.43 (1.07–1.91) <sup>a</sup>	1.98 (1.51–2.60) <sup>d</sup>	1.67 (1.27–2.19) <sup>d</sup>	1.65 (1.15–2.36) <sup>b</sup>
Tb.N	1.81 (1.41–2.17) <sup>d</sup>	1.68 (1.40–2.02) <sup>d</sup>	1.63 (1.31–2.03) <sup>d</sup>	1.96 (1.56–2.46) <sup>d</sup>	1.80 (1.43–2.26) <sup>d</sup>	1.80 (1.38–2.36) <sup>d</sup>
Tb.Th	1.28 (1.04–1.59) <sup>a</sup>	1.09 (0.88–1.35)	0.85 (0.67–1.09)	1.38 (1.05–1.80) <sup>a</sup>	1.21 (0.85–1.57)	0.89 (0.65–1.22)
Tb.Sp	1.53 (1.37–1.70) <sup>d</sup>	1.42 (1.27–1.59) <sup>d</sup>	1.37 (1.19–1.58) <sup>d</sup>	1.61 (1.41–1.85) <sup>d</sup>	1.48 (1.29–1.70) <sup>d</sup>	1.46 (1.24–1.73) <sup>d</sup>
Tb.Sp.SD	1.25 (1.16–1.34) <sup>d</sup>	1.20 (1.11–1.30) <sup>d</sup>	1.15 (1.05–1.26) <sup>c</sup>	1.27 (1.17–1.38) <sup>d</sup>	1.22 (1.12–1.34) <sup>d</sup>	1.18 (1.06–1.31) <sup>c</sup>
Conn. D	1.96 (1.56–2.47) <sup>d</sup>	1.77 (1.40–2.23) <sup>d</sup>	1.67 (1.27–2.19) <sup>d</sup>	2.23 (1.66–3.01) <sup>d</sup>	1.95 (1.46–2.62) <sup>d</sup>	1.93 (1.37–2.72) <sup>d</sup>
Stiffness	1.63 (1.31–2.03) <sup>d</sup>	1.32 (1.04–1.68) <sup>a</sup>	0.90 (0.62–1.30)	1.77 (1.34–2.35) <sup>d</sup>	1.36 (1.01–1.84) <sup>a</sup>	0.97 (0.61–1.56)
Fail. load	1.62 (1.30–2.03) <sup>d</sup>	1.33 (1.05–1.69) <sup>a</sup>	0.94 (0.66–1.35)	1.76 (1.33–2.34) <sup>d</sup>	1.37 (1.01–1.86) <sup>a</sup>	1.02 (0.65–1.61)
Tibia	(n/N = 101/777)			(n/N = 71/771)		
Tt.vBMD	1.73 (1.40–2.12) <sup>d</sup>	1.48 (1.19–1.85) <sup>d</sup>	1.18 (0.90–1.54)	1.79 (1.38–2.33) <sup>d</sup>	1.50 (1.13–1.97) <sup>c</sup>	1.09 (0.78–1.53)
Ct.vBMD	1.58 (1.36–1.83) <sup>d</sup>	1.34 (1.13–1.59) <sup>d</sup>	1.19 (0.98–1.45)	1.61 (1.32–1.95) <sup>d</sup>	1.29 (1.02–1.62) <sup>d</sup>	1.08 (0.83–1.41)
Ct.Th	1.73 (1.41–2.12) <sup>d</sup>	1.47 (1.18–1.82) <sup>d</sup>	1.23 (0.97–1.57)	1.72 (1.34–2.22) <sup>d</sup>	1.41 (1.08–1.84) <sup>a</sup>	1.10 (0.81–1.49)
Tb.vBMD	1.48 (1.21–1.80) <sup>d</sup>	1.30 (1.06–1.59) <sup>a</sup>	1.02 (0.80–1.30)	1.56 (1.22–2.00) <sup>d</sup>	1.37 (1.06–1.76) <sup>a</sup>	1.01 (0.74–1.37)
Tb.N	1.31 (1.09–1.59) <sup>c</sup>	1.26 (1.03–1.53) <sup>a</sup>	1.01 (0.81–1.27)	1.44 (1.14–1.82) <sup>c</sup>	1.40 (1.09–1.80) <sup>b</sup>	1.11 (0.84–1.47)
Tb.Th	1.28 (1.04–1.57) <sup>a</sup>	1.12 (0.91–1.37)	1.00 (0.82–1.23)	1.30 (1.01–1.67) <sup>a</sup>	1.10 (0.85–1.42)	0.94 (0.72–1.22)
Tb.Sp	1.26 (1.11–1.42) <sup>d</sup>	1.24 (1.07–1.43) <sup>c</sup>	1.05 (0.87–1.27)	1.31 (1.14–1.51) <sup>d</sup>	1.33 (1.12–1.58) <sup>d</sup>	1.13 (0.90–1.41)
Tb.Sp.SD	1.12 (1.04–1.20) <sup>c</sup>	1.13 (1.04–1.23) <sup>c</sup>	1.05 (0.94–1.19)	1.14 (1.04–1.22) <sup>c</sup>	1.16 (1.05–1.27) <sup>c</sup>	1.08 (0.94–1.24)
Conn. D	1.28 (1.04–1.57) <sup>a</sup>	1.21 (0.98–1.50)	1.02 (0.81–1.23)	1.45 (1.11–1.90) <sup>b</sup>	1.40 (1.06–1.83) <sup>a</sup>	1.15 (0.86–1.55)
Stiffness	1.81 (1.45–2.25) <sup>d</sup>	1.48 (1.17–1.87) <sup>c</sup>	1.12 (0.82–1.52)	1.90 (1.44–2.51) <sup>d</sup>	1.47 (1.09–1.99) <sup>a</sup>	0.99 (0.67–1.46)
Fail. load	1.79 (1.44–2.23) <sup>d</sup>	1.46 (1.15–1.85) <sup>c</sup>	1.10 (0.81–1.50)	1.89 (1.43–2.50) <sup>d</sup>	1.47 (1.09–1.99) <sup>a</sup>	0.99 (0.67–1.46)

BMI = body mass index; aBMD = areal bone mineral density; N = number of men who had valid HR-pQCT measurement for this skeletal site and were followed up for at least 1 year (eg, 751 for distal radius); n = number of men who sustained at least one incident fragility fracture in this group; Tt.vBMD = total volumetric bone mineral density; Ct.vBMD = cortical volumetric bone mineral density; Ct.Th = cortical thickness; Tb.vBMD = trabecular volumetric bone mineral density; Tb.N = trabecular number; Tb.Th = trabecular thickness; Tb.Sp = trabecular separation; Tb.Sp.SD = standard deviation of the trabecular separation; Conn. D = connectivity density; Fail. load = failure load.

<sup>a</sup>p < 0.05.

<sup>b</sup>p < 0.01.

<sup>c</sup>p < 0.005.

<sup>d</sup>p < 0.001.

<sup>e</sup>HR and 95% CI are calculated per 1 SD decrease except for Tb.Sp and Tb.Sp.SD, which are calculated per 1 SD increase.

<sup>f</sup>Distal radius aBMD for distal radius; total hip aBMD for distal tibia.

**Table 3.** Association Between HR-pQCT Parameters and the Risk of Incident Radiographic Vertebral Fracture or Incident Nonvertebral Fracture in Older Men

	Incident vertebral fractures			Incident nonvertebral fractures		
	Unadjusted	Adjusted for age, BMI, prior falls and fractures	Additionally adjusted for aBMD <sup>f</sup>	Unadjusted	Adjusted for age, BMI, prior falls and fractures	Additionally adjusted for aBMD <sup>f</sup>
	HR per SD (95% CI) <sup>e</sup>			HR per SD (95% CI) <sup>e</sup>		
Radius	(n/N = 46/616)			(n/N = 65/751)		
Tt.vBMD	1.98 (1.42–2.77) <sup>d</sup>	1.41 (1.00–2.00) <sup>a</sup>	1.61 (0.93–2.76)	1.75 (1.32–2.31) <sup>d</sup>	1.52 (1.12–2.06) <sup>b</sup>	1.18 (0.76–1.83)
Ct.vBMD	1.44 (1.10–1.88) <sup>b</sup>	0.90 (0.65–1.24)	0.69 (0.46–1.05)	1.52 (1.21–1.92) <sup>d</sup>	1.31 (1.01–1.72) <sup>a</sup>	1.03 (0.73–1.45)
Ct.Th	1.68 (1.22–2.31) <sup>c</sup>	1.09 (0.78–1.53)	0.92 (0.57–1.46)	1.64 (1.24–2.16) <sup>d</sup>	1.39 (1.03–1.89) <sup>a</sup>	1.05 (0.71–1.56)
Tb.vBMD	1.96 (1.42–2.69) <sup>d</sup>	1.58 (1.16–2.16) <sup>d</sup>	1.87 (1.22–2.84) <sup>c</sup>	1.68 (1.29–2.19) <sup>d</sup>	1.49 (1.13–1.96) <sup>c</sup>	1.23 (0.85–1.78)
Tb.N	1.87 (1.41–2.45) <sup>d</sup>	1.65 (1.26–2.16) <sup>d</sup>	1.78 (1.30–2.44) <sup>d</sup>	1.68 (1.34–2.11) <sup>d</sup>	1.60 (1.27–2.02) <sup>d</sup>	1.46 (1.11–1.93) <sup>b</sup>
Tb.Th	1.45 (1.05–2.00) <sup>a</sup>	1.17 (0.85–1.52)	1.12 (0.77–1.63)	1.24 (0.95–1.62)	1.06 (0.81–1.38)	0.79 (0.58–1.07)
Tb.Sp	1.57 (1.33–1.85) <sup>d</sup>	1.36 (1.14–1.62) <sup>d</sup>	1.39 (1.14–1.70) <sup>d</sup>	1.45 (1.27–1.66) <sup>d</sup>	1.38 (1.19–1.59) <sup>d</sup>	1.29 (1.07–1.55) <sup>b</sup>
Tb.Sp.SD	1.34 (1.15–1.56) <sup>d</sup>	1.20 (1.01–1.43) <sup>a</sup>	1.20 (0.99–1.44)	1.24 (1.14–1.35) <sup>d</sup>	1.20 (1.10–1.32) <sup>d</sup>	1.14 (1.02–1.27) <sup>a</sup>
Conn. D	2.27 (1.61–3.22) <sup>d</sup>	1.89 (1.35–2.63) <sup>d</sup>	2.12 (1.42–3.15) <sup>d</sup>	1.71 (1.28–2.27) <sup>d</sup>	1.57 (1.18–2.09) <sup>c</sup>	1.36 (0.97–1.91)
Stiffness	1.67 (1.21–2.31) <sup>c</sup>	1.17 (0.83–1.65)	1.07 (0.66–1.75)	1.63 (1.23–2.16) <sup>d</sup>	1.36 (1.01–1.86) <sup>a</sup>	0.86 (0.54–1.37)
Fail. load	1.65 (1.19–2.28) <sup>c</sup>	1.18 (0.84–1.67)	1.10 (0.69–1.76)	1.22 (1.22–2.15) <sup>d</sup>	1.37 (1.01–1.86) <sup>a</sup>	0.89 (0.57–1.40)
Tibia	(n/N = 48/628)			(n/N = 67/777)		
Tt.vBMD	1.85 (1.35–2.54) <sup>d</sup>	1.50 (1.07–2.08) <sup>a</sup>	1.17 (0.78–1.74)	1.73 (1.33–2.25) <sup>d</sup>	1.53 (1.15–2.03) <sup>c</sup>	1.21 (0.85–1.71)
Ct.vBMD	1.52 (1.20–1.92) <sup>d</sup>	1.11 (0.84–1.47)	0.95 (0.71–1.27)	1.59 (1.35–1.89) <sup>d</sup>	1.42 (1.16–1.75) <sup>d</sup>	1.28 (1.01–1.62) <sup>a</sup>
Ct.Th	1.69 (1.24–2.30) <sup>d</sup>	1.30 (0.94–1.79)	1.05 (0.74–1.48)	1.83 (1.42–2.36) <sup>d</sup>	1.62 (1.23–2.13) <sup>d</sup>	1.37 (1.01–1.87) <sup>a</sup>
Tb.vBMD	1.66 (1.24–2.22) <sup>d</sup>	1.45 (1.07–1.95) <sup>a</sup>	1.16 (0.81–1.67)	1.42 (1.11–1.81) <sup>b</sup>	1.26 (0.97–1.64)	0.96 (0.70–1.32)
Tb.N	1.58 (1.20–2.07) <sup>d</sup>	1.45 (1.09–1.92) <sup>a</sup>	1.20 (0.86–1.67)	1.16 (0.92–1.47)	1.12 (0.88–1.44)	0.87 (0.66–1.16)
Tb.Th	1.30 (0.95–1.76)	1.18 (0.86–1.62)	1.04 (0.76–1.44)	1.33 (1.03–1.72) <sup>a</sup>	1.15 (0.89–1.49)	1.03 (0.78–1.35)
Tb.Sp	1.35 (1.16–1.57) <sup>d</sup>	1.32 (1.10–1.59) <sup>c</sup>	1.17 (0.92–1.49)	1.16 (0.96–1.39)	1.12 (0.92–1.38)	0.90 (0.69–1.17)
Tb.Sp.SD	1.13 (1.03–1.24) <sup>b</sup>	1.14 (1.01–1.28) <sup>a</sup>	1.07 (0.91–1.25)	1.09 (0.98–1.21)	1.10 (0.97–1.24)	0.99 (0.82–1.20)
Conn. D	1.65 (1.19–2.30) <sup>c</sup>	1.50 (1.08–2.08) <sup>a</sup>	1.26 (0.88–1.79)	1.10 (0.85–1.41)	1.06 (0.82–1.37)	0.86 (0.65–1.15)
Stiffness	1.86 (1.34–2.59) <sup>d</sup>	1.35 (0.94–1.93)	0.90 (0.57–1.43)	1.96 (1.49–2.58) <sup>d</sup>	1.68 (1.24–2.28) <sup>d</sup>	1.39 (0.93–2.07)
Fail. load	1.86 (1.34–2.59) <sup>d</sup>	1.34 (0.94–1.92)	0.90 (0.57–1.42)	1.92 (1.46–2.53) <sup>d</sup>	1.65 (1.22–2.24) <sup>c</sup>	1.34 (0.90–1.99)

BMI = body mass index; aBMD = areal bone mineral density; N = number of men who had valid HR-pQCT measurement for this skeletal site and, for vertebral fractures, had at least one follow-up lumbar spine DXA scan (eg, 616 for distal radius) or, for nonvertebral fractures (eg, 751 for distal radius), were followed up for at least one year; n = number of men who sustained at least one incident fragility fracture in this group; Tt.vBMD = total volumetric bone mineral density; Ct.vBMD = cortical volumetric bone mineral density; Ct.Th = cortical thickness; Tb.vBMD = trabecular volumetric bone mineral density; Tb.N = trabecular number; Tb.Th = trabecular thickness; Tb.Sp = trabecular separation; Tb.Sp.SD = standard deviation of the trabecular separation; Conn. D = connectivity density; Fail. load = failure load.

<sup>a</sup>p < 0.05.

<sup>b</sup>p < 0.01.

<sup>c</sup>p < 0.005.

<sup>d</sup>p < 0.001.

<sup>e</sup>HR and 95% CI are calculated per 1 SD decrease except for Tb.Sp and Tb.Sp.SD, which are calculated per 1 SD increase.

<sup>f</sup>Distal radius aBMD for distal radius; total hip aBMD for distal tibia.

## Nonvertebral fractures

Median follow-up to the first nonvertebral fracture was 3.7 years (IQR 2.2–5.6). In the unadjusted models, most distal radius and some distal tibia measures were associated with the risk of nonvertebral fracture. Among 751 men with valid distal radius scans, 65 had nonvertebral fractures. After adjustment for age, BMI, falls, and fractures, nearly all distal radius HR-pQCT measures were associated with the nonvertebral fracture risk. After adjustment for distal radius aBMD, Tb.N, Tb.Sp, and Tb.Sp.SD remained significant. The results were similar after adjustment for total hip aBMD, eg, Tb.N: HR = 1.42 per SD, 95% CI 1.08–1.87,  $p < 0.05$ . In 777 men with valid tibia scan, low Tt.vBMD, Ct.vBMD, Ct.Th, stiffness, and failure load were associated with higher nonvertebral fracture risk (67 men). After adjustment for hip aBMD, cortical measures remained associated weakly significantly with higher fracture risk.

### Sensitivity analysis for the trabecular measures of distal radius

Distal radius low Tb.N was associated with higher risk of any fracture in 592 men without prior fracture (HR = 1.47 per SD, 95% CI 1.14–1.91,  $p < 0.005$ ). Similar patterns were found for fracture groups, eg, major osteoporotic fracture: HR = 1.70 per SD, 95% CI 1.24–2.34,  $p < 0.005$ . Lower Tb.N was associated with higher risk of any fracture in 591 men reporting no falls during the year prior to baseline (HR = 1.61 per SD, 95% CI 1.25–2.06,  $p < 0.001$ ). Similar patterns were found for fracture subgroups, eg, vertebral fracture: HR = 2.07 per SD, 95% CI 1.42–3.02,  $p < 0.001$ . Lower Tb.N was associated with higher risk of any fracture in 152 men who had fractures before the study (HR = 2.12 per SD, 95% CI 1.41–3.20,  $p < 0.001$ ) and in 146 men reporting falls (HR = 1.63 per SD, 95% CI 1.01–2.61,  $p < 0.05$ ). Point estimates were similar in fracture subgroups but not always significant because of insufficient power. The associations were similar, though weaker, for Tb.Sp and Conn. D. For instance, high Tb.Sp was associated with higher risk of any fracture in men without prior fracture (HR = 1.33 per SD, 95% CI 1.09–1.62,  $p < 0.005$ ) and in men who had prior fractures (HR = 1.49 per SD, 95% CI 1.19–1.87,  $p < 0.001$ ). Low Conn. D Sp was associated with higher risk of any fracture in men without prior fracture (HR = 1.53 per SD, 95% CI 1.24–2.10,  $p < 0.01$ ) and in men who had prior fractures (HR = 2.15 per SD, 95% CI 1.24–3.74,  $p < 0.01$ ).

The most discriminating threshold for all fractures (found by Youden's index) was 1.85/mm for Tb.N (sensitivity 73%, specificity 54%) and 0.943 g/cm<sup>2</sup> for hip aBMD (sensitivity 67%, specificity 55%) (Fig. 2). Men were divided into four groups using these thresholds (Table 4). The risk of all types of fracture was four- to sixfold higher in men who had hip aBMD and Tb.N below the thresholds versus men who were above the thresholds for both measures. The risks of any, vertebral, and major osteoporotic fractures were increased in men with low Tb.N even in men with hip aBMD  $\geq 0.943$  g/cm<sup>2</sup>.

Similar results were found for distal radius Tb.Sp and Conn. D. The most discriminating value for distal radius Tb.Sp was 0.48 mm (sensitivity 64%, specificity 62%). Men with high Tb.Sp ( $>0.48$  mm) and low hip aBMD had higher all fracture risk versus the reference (Tb.Sp  $\leq 0.48$  mm, hip aBMD  $\geq 0.943$  g/cm<sup>2</sup>): HR = 4.10, 95% CI 2.22–7.57,  $p < 0.001$ . The threshold for Conn. D was 3.59 (sensitivity 65%, specificity 55%). Men with low Conn. D ( $<3.59$ ) and low aBMD had higher all-fracture risk versus the reference (Conn. D  $\geq 3.59$ , aBMD  $\geq 0.943$  g/cm<sup>2</sup>): HR = 3.50, 95% CI 1.89–6.50,  $p < 0.001$ .

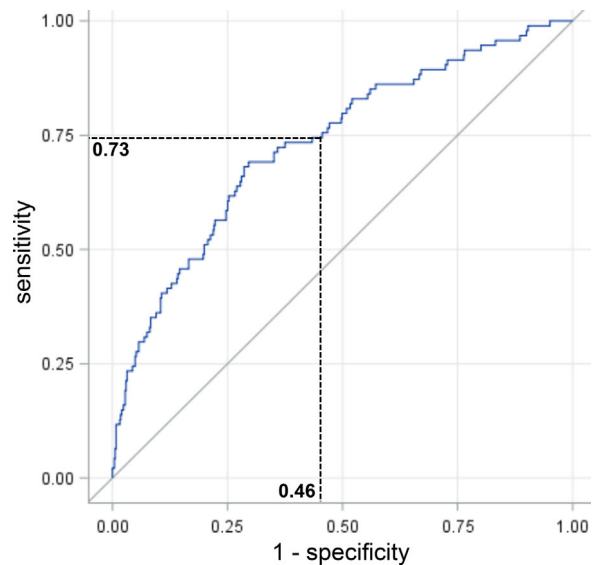


**Fig. 2.** Calculation of Youden's index – area under the curve presenting the association between distal radius Tb.N and fracture risk. Sensitivity (73%) and specificity (54%,  $0.54 = 1 - 0.46$ ) correspond to the most discriminating threshold, Tb.N = 1.85.

### Distal radius trabecular measured and improvement of fracture prediction

The adjustment for Tb.N did not change the estimated risk of any fracture in men who did not sustain fracture (0.1%, 95% CI -0.4% to 0.7%) but increased the estimated risk in men who had fracture (4.2%, 95% CI 2.1% to 6.4%). Thus, the adjustment for Tb.N increased the estimated fracture risk more in men who sustained the fracture (diff = 4.1%, 95% CI 1.9% to 6.3%,  $p < 0.001$ ). The adjustment for Tb.N increased the estimated risk of different types of fracture in those who sustained the fracture but had no impact in those who did not. Thus, the adjustment for Tb.N improved the discrimination between men who did or did not have the fracture for all fracture types: 5.4% (95% CI 3.6% to 7.0%,  $p < 0.001$ ) for major osteoporotic fractures, 3.9% for vertebral fracture (95% CI 1.2% to 6.6%,  $p < 0.01$ ), 2.7% for the nonvertebral fracture (95% CI 0.4% to 4.9%,  $p < 0.05$ ). Similarly, distal radius Tb.Sp and Conn. D improved the discrimination between men who did or did not have the fracture irrespective of the fracture type, eg, for major osteoporotic fracture: 3.6% (95% CI 0.1% to 7.2%,  $p < 0.01$ ) and 3.6% (95% CI 0.1% to 6.1%,  $p < 0.005$ ), respectively.

By contrast, no HR-pQCT parameter increased significantly the AUC for any type of fracture (Harrell's diagnostic, differences between AUCs  $\leq 0.02$ ,  $p > 0.10$ ).

## Discussion

In a prospectively followed cohort of older men, poor bone microarchitecture was associated with higher risk of fracture, vertebral and nonvertebral, after adjustment for age, BMI, falls, and fractures. Adjustment for aBMD weakened the associations; however, distal radius Tb.N and Conn. D (and more weakly, its inverse Tb.Sp and Tb.Sp.SD) were associated significantly with all types of fractures. Lower distal radius Tb.N was also associated

**Table 4.** Contribution of Low Distal Radius Trabecular Number (Tb.N) and Low Total Hip Areal Bone Mineral Density (aBMD) to the Risk of Fracture

Distal radius Tb.N	Total hip aBMD	Incidence (per 1000 person-years)	HR (95% CI)	p Value
<b>All fractures</b>				
≥1.85 /mm	≥0.943 g/cm <sup>2</sup>	7.56	1.00	
≥1.85 /mm	<0.943 g/cm <sup>2</sup>	18.58	1.88 (0.87–4.08)	0.11
<1.85 /mm	≥0.943 g/cm <sup>2</sup>	21.18	2.43 (1.15–5.14)	<0.05
<1.85 /mm	<0.943 g/cm <sup>2</sup>	35.61	4.34 (2.29–8.24)	<0.001
<b>Major osteoporotic fracture</b>				
≥1.85 /mm	≥0.943 g/cm <sup>2</sup>	3.78	1.00	
≥1.85 /mm	<0.943 g/cm <sup>2</sup>	12.78	1.91 (0.67–5.43)	0.22
<1.85 /mm	≥0.943 g/cm <sup>2</sup>	11.77	3.21 (1.21–8.53)	<0.05
<1.85 /mm	<0.943 g/cm <sup>2</sup>	22.42	5.71 (2.42–13.47)	<0.001
<b>Vertebral fractures</b>				
≥1.85 /mm	≥0.943 g/cm <sup>2</sup>	2.49	1.00	
≥1.85 /mm	<0.943 g/cm <sup>2</sup>	11.58	2.71 (0.77–9.55)	0.12
<1.85 /mm	≥0.943 g/cm <sup>2</sup>	13.20	6.19 (1.89–20.29)	<0.005
<1.85 /mm	<0.943 g/cm <sup>2</sup>	19.73	6.32 (2.12–18.87)	<0.001
<b>Nonvertebral fractures</b>				
≥1.85 /mm	≥0.943 g/cm <sup>2</sup>	5.38	1.00	
≥1.85 /mm	<0.943 g/cm <sup>2</sup>	12.75	2.04 (0.79–5.25)	0.14
<1.85 /mm	≥0.943 g/cm <sup>2</sup>	10.38	1.30 (0.46–3.65)	0.62
<1.85 /mm	<0.943 g/cm <sup>2</sup>	22.40	4.34 (1.98–9.50)	<0.001

The thresholds of distal radius Tb.N (1.85 /mm) and of total hip aBMD (0.943 g/cm<sup>2</sup>) were established using the Youden's index. The models are adjusted for age, weight, prior falls, and prior fractures.

with higher risk of vertebral and major osteoporotic fracture in men with higher aBMD. Finally, the addition of distal radius Tb.N improved fracture prediction in comparison with the reference model (age, weight, prior falls and fractures, aBMD).

Our data confirm that poor bone microarchitecture is associated with fracture risk irrespective of aBMD. Men with vertebral fractures had lower trabecular number assessed in bone biopsy versus men with similar aBMD but without fracture.<sup>(31)</sup> Other cross-sectional studies showed that subjects with fragility fractures had poorer bone microarchitecture assessed by HR-pQCT versus those without fracture, even after adjustment for aBMD.<sup>(17–19,32–34)</sup> These relations were found in men and women, for vertebral and, to a lesser extent, nonvertebral fractures. Women with vertebral fractures had poorer bone microarchitecture, especially of trabecular bone, versus those with nonvertebral fractures.<sup>(35)</sup> These data are consistent with experimental results showing the importance of bone microarchitecture for bone strength.<sup>(36,37)</sup>

Distal radius HR-pQCT parameters were more strongly associated with the fracture risk compared with distal tibia. This is in line with some,<sup>(24,38–40)</sup> but not all,<sup>(19,32,34,35,40,41)</sup> studies. However, these results cannot be extrapolated on ours. Few prospective studies assessed fracture prediction by the bone HR-pQCT measures in postmenopausal women.<sup>(21,42)</sup> In these studies, both trabecular and cortical parameters predicted fractures; however, point estimates were higher and the associations stronger for distal radius. Radius is a non-weight-bearing site, whereas tibia is protected by body weight. Thus, distal radius may better reflect the effect of various determinants of bone turnover and bone strength than the tibia. However, data do not support this speculation. In our cohort, smoking and high C-reactive protein level were associated with poorer bone microarchitecture at distal radius but not distal tibia.<sup>(43,44)</sup> By contrast, low sex steroid levels and secondary hyperparathyroidism were

associated with similar deterioration of bone microarchitecture at both skeletal sites.<sup>(45,46)</sup>

Trabecular measures predicted fractures better than cortical ones and better than composite  $\mu$ FEA measures of bone strength determined mainly by cortical bone status. Trabecular bone contributes largely to bone strength in compression,<sup>(36,37)</sup> and 60% of fractures in our cohort are due to compression (vertebra, distal radius, trochanter). It may also contribute to bone strength in the meta- and epiphysis, eg, in fractures of proximal humerus and proximal or distal tibia. In cross-sectional studies, both poor cortical and trabecular measures were found in subjects with fragility fractures.<sup>(20,33,35,38,40,41,47)</sup> In some studies, the links were stronger for cortical than trabecular measures.<sup>(19,39,48)</sup> By contrast, in the prospective studies, cortical parameters lost significance after adjustment for aBMD.<sup>(21,42)</sup>

Cortical bone has higher mass than trabecular bone and is the main determinant of aBMD. This applies for cross-sectional and prospective studies and does not explain the difference between them. Cortical bone confers strength for bending and torsion and its mass represents a higher fraction of mass in long bones versus vertebral bodies. It may result in a stronger link of cortical measures with nonvertebral versus vertebral fractures. However, clinical studies do not support this speculation.<sup>(19,35)</sup> A cross-sectional analysis may be influenced by bone loss developing after fracture due to low physical activity. In experimental and clinical studies, unloading (hindlimb suspension) and weightlessness result in a similar bone loss in cortical and trabecular compartments.<sup>(49,50)</sup> The strong fracture prediction by Tb.N in both sexes is not explained by different age-related bone loss in these compartments either. In both sexes, the age-related decrease in trabecular variables is not greater than that in cortical ones.<sup>(51,52)</sup> Inaccurate assessment of cortical bone in the oldest men may weaken predictive value of cortical parameters for fracture prediction in older men.



However, the fraction of load borne by cortical bone decreases with age in men.<sup>(52)</sup> Moreover, during re-ambulation after long-term space flight, distal tibia cortical bone recovered, but trabecular bone and failure load did not.<sup>(44)</sup> These findings also confirm the importance of trabecular bone for bone strength.

The adjustment for distal radius trabecular measures increased the predicted fracture probability assessed by IDI, but not by Harrell's statistics, in men who subsequently sustained fractures. By contrast, it had no impact on the estimated fracture probability in men who did not sustain fractures. Biver and colleagues showed that distal radius failure load improved fracture prediction in older women.<sup>(36)</sup> However, in the Gerico study, the statistical model was not adjusted for prior falls and fractures. Failure load is a composite parameter reflecting bone status in the cortical and trabecular compartments. Despite the differences, both studies show that the evaluation of bone microarchitecture at distal radius may improve estimation of fracture probability. However, in men, the improvement of the fracture probability estimation is limited to the IDI algorithm and does not seem to be clinically relevant.

Our study has strengths. It assesses prospectively fracture prediction by HR-pQCT measures in older men. The incident fractures were confirmed by spine scans or health professional. We checked site and circumstances of fractures. The statistical models were adjusted for other risk factors. Tb.N is the inverse of the directly measured Tb.Sp. We recognize limitations. This single-center cohort consists of home-dwelling, mainly white men. Elderly volunteers in research studies are healthier than general population of similar age. The results cannot be extrapolated to women, younger men, other ethnicities, or patients with secondary osteoporosis. Tb.Th, Tb.Sp.SD, and Ct.Th are calculated. Partial volume effect may render assessment of microarchitectural parameters inaccurate. The assessment of cortical bone may be erroneous in the oldest men with thin cortex.  $\mu$ FEA measures reflect bone strength to compression, not other deformations. HR-pQCT does not account for intrinsic deterioration of bone (microdamage, mineral imperfections, abnormal posttranslational modifications of bone proteins). Prior falls and nonvertebral fractures were self-reported and not checked. Because medical records were not scrutinized for incident fractures, false negatives are possible. Incident vertebral fractures were assessed only in men who returned for a follow-up visit and had DXA. This may underestimate the number of incident vertebral fractures, especially that sicker men may have higher vertebral fracture incidence. In an observational study, residual confounding is possible.

Overall, poor bone microarchitecture is associated with higher fracture risk after adjustment for age, BMI, prior falls, and fractures. After further adjustment for aBMD, distal radius trabecular parameters (Tb.N, Tb.Sp, Conn. D) remained significantly associated with higher fracture risk. These trabecular measures were associated with high risk of fracture in various low-risk groups (men without fracture, men not reporting fall, men with higher aBMD). The assessment of distal radius trabecular measures may improve the estimation of fracture probability in older men. However, this improvement is small and not clinically relevant. These data need confirmation, but they provide interesting hints. We need more studies on the determinants of trabecular bone (genetic factors, hormones, lifestyle) and on its role as a determinant of bone strength. Our data suggest that preservation of trabeculae (by antiresorptive agents) or their restoration (by bone formation-stimulating agents) may play an important role in fracture prevention in older men.

## Disclosures

All authors state that they have no conflicts of interest.

## Acknowledgments

This study was supported by grants from the pharmaceutical company Roche (Basel, Switzerland), Abondement ANVAR (E1482.042), Agence Nationale de la Recherche (ANR-07-PHYSIO-023-01), and Hospices Civils de Lyon (50564) to PS and RC. None of the funding organizations had access to the data nor were involved in any analyses concerning this study.

Authors' roles: PS was responsible for the study, performed initial questionnaire and the follow-up of the incident fractures, made the statistical analyses and wrote the manuscript. SB was responsible for the acquisition and quality control of all the HRpQCT scans in the cohort. SB and RC reviewed the manuscript and contributed to the interpretation of the data and to the discussion. PS and RC obtained the funding for the study. PS is the guarantor of this work, had full access to all the data in the study and takes responsibility for the integrity and the accuracy of the data analysis.

## References

1. Kontis V, Bennett JE, Mathers CD, Li G, Foreman K, Ezzati M. Future life expectancy in 35 industrialised countries: projections with a Bayesian model ensemble. *Lancet*. 2017;389:1323–35.
2. Bliuc D, Nguyen ND, Milch VE, Nguyen TV, Eisman JA, Center JR. Mortality risk associated with low-trauma osteoporotic fracture and subsequent fracture in men and women. *JAMA*. 2009;301:513–21.
3. Schuit SC, van der Klift M, Weel AE, et al. Fracture incidence and association with bone mineral density in elderly men and women: the Rotterdam Study. *Bone*. 2004;34:195–202.
4. Szulc P, Munoz F, Duboeuf F, Marchand F, Delmas PD. Bone mineral density predicts osteoporotic fractures in elderly men: the MINOS study. *Osteoporos Int*. 2005;16:1184–92.
5. Szulc P, Montella A, Delmas PD. High bone turnover is associated with accelerated bone loss but not with increased fracture risk in men aged 50 and over: the prospective MINOS study. *Ann Rheum Dis*. 2008;67:1249–55.
6. Orwoll ES, Lapidus J, Wang PY, et al. The limited clinical utility of testosterone, estradiol, and sex hormone binding globulin measurements in the prediction of fracture risk and bone loss in older men. *J Bone Miner Res*. 2017;32:633–40.
7. Bauer DC, Ewing SK, Cauley JA, Ensrud KE, Cummings SR, Orwoll ES. Quantitative ultrasound predicts hip and non-spine fracture in men: the MrOS study. *Osteoporos Int*. 2007;18:771–7.
8. Black DM, Bouxsein ML, Marshall LM, et al. Proximal femoral structure and the prediction of hip fracture in men: a large prospective study using QCT. *J Bone Miner Res*. 2008;23:1326–33.
9. Ettinger B, Ensrud KE, Blackwell T, Curtis JR, Lapidus JA, Orwoll ES. Performance of FRAX in a cohort of community-dwelling, ambulatory older men: the Osteoporotic Fractures in Men (MrOS) study. *Osteoporos Int*. 2013;24:1185–93.
10. Pothuau L, Carceller P, Hans D. Correlations between grey-level variations in 2D projection images (TBS) and 3D microarchitecture: applications in the study of human trabecular bone microarchitecture. *Bone*. 2008;42:775–87.
11. Leslie WD, Aubry-Rozier B, Lix LM, Morin SN, Majumdar SR, Hans D. Spine bone texture assessed by trabecular bone score (TBS) predicts osteoporotic fractures in men: the Manitoba Bone Density Program. *Bone*. 2014;67:10–4.
12. McCloskey EV, Odén A, Harvey NC, et al. A meta-analysis of trabecular bone score in fracture risk prediction and its relationship to FRAX. *J Bone Miner Res*. 2016;31:940–8.

13. Schousboe JT, Vo T, Taylor BC, et al. Prediction of incident major osteoporotic and hip fractures by trabecular bone score (TBS) and prevalent radiographic vertebral fracture in older men. *J Bone Miner Res.* 2016;31:690–7.
14. Schousboe JT, Vo TN, Langsetmo L, et al. Association of trabecular bone score (TBS) with incident clinical and radiographic vertebral fractures adjusted for lumbar spine BMD in older men: a prospective cohort study. *J Bone Miner Res.* 2017;32:1554–8.
15. Iki M, Fujita Y, Tamaki J, et al. Trabecular bone score may improve FRAX<sup>®</sup> prediction accuracy for major osteoporotic fractures in elderly Japanese men: the Fujiwara-kyo Osteoporosis Risk in Men (FORMEN) cohort study. *Osteoporos Int.* 2015;26:1841–8.
16. Bouxsein ML, Seeman E. Quantifying the material and structural determinants of bone strength. *Best Pract Res Clin Rheumatol.* 2009;23:741–53.
17. Sornay-Rendu E, Boutroy S, Munoz F, Delmas PD. Alterations of cortical and trabecular architecture are associated with fractures in postmenopausal women, partially independent of decreased BMD measured by DXA: the OFELY study. *J Bone Miner Res.* 2007;22:425–33.
18. Vico L, Zouch M, Amirouche A, et al. High-resolution pQCT analysis at the distal radius and tibia discriminates patients with recent wrist and femoral neck fractures. *J Bone Miner Res.* 2008;23:1741–50.
19. Szulc P, Boutroy S, Vilayphiou N, Chaitou A, Delmas PD, Chapurlat R. Cross-sectional analysis of the association between fragility fractures and bone microarchitecture in older men: the STRAMBO study. *J Bone Miner Res.* 2011;26:1358–67.
20. Sundh D, Mellström D, Nilsson M, Karlsson M, Ohlsson C, Lorentzon M. Increased cortical porosity in older men with fracture. *J Bone Miner Res.* 2015;30:1692–700.
21. Sornay-Rendu E, Boutroy S, Duboeuf F, Chapurlat RD. Bone microarchitecture assessed by HR-pQCT as predictor of fracture risk in postmenopausal women: the OFELY study. *J Bone Miner Res.* 2017;32:1243–51.
22. Chaitou A, Boutroy S, Vilayphiou N, et al. Association between bone turnover rate and bone microarchitecture in men: the STRAMBO study. *J Bone Miner Res.* 2010;25:2133–23.
23. Pialat JB, Burghardt AJ, Sode M, Link TM, Majumdar S. Visual grading of motion induced image degradation in high resolution peripheral computed tomography: impact of image quality on measures of bone density and micro-architecture. *Bone.* 2012;50:111–8.
24. Boutroy S, Bouxsein ML, Munoz F, Delmas PD. In vivo assessment of trabecular bone microarchitecture by high-resolution peripheral quantitative computed tomography. *J Clin Endocrinol Metab.* 2005;90:6508–15.
25. van Rietbergen B, Weinans H, Huiskes R, Odgaard A. A new method to determine trabecular bone elastic properties and loading using micromechanical finite-element models. *J Biomech.* 1995;28:69–81.
26. Turner CH, Rho J, Takano Y, Tsui TY, Pharr GM. The elastic properties of trabecular and cortical bone tissues are similar: results from two microscopic measurement techniques. *J Biomech.* 1999;32:437–41.
27. Chiu J, Robinovitch SN. Prediction of upper extremity impact forces during falls on the outstretched hand. *J Biomech.* 1998;31:1169–76.
28. Boutroy S, Hans D, Sornay-Rendu E, Vilayphiou N, Winzenrieth R, Chapurlat R. Trabecular bone score improves fracture risk prediction in non-osteoporotic women: the OFELY study. *Osteoporos Int.* 2013;24:77–85.
29. Youden WJ. Index for rating diagnostic tests. *Cancer.* 1950;3:32–5.
30. Pencina MJ, D'Agostino RB Sr, D'Agostino RB Jr, Vasan RS. Evaluating the added predictive ability of a new marker: from area under the ROC curve to reclassification and beyond. *Stat Med.* 2008;27:157–72.
31. Legrand E, Chappard D, Pascaretti C, et al. Trabecular bone microarchitecture, bone mineral density, and vertebral fractures in male osteoporosis. *J Bone Miner Res.* 2000;15:13–9.
32. Stein EM, Liu XS, Nickolas TL, et al. Abnormal microarchitecture and stiffness in postmenopausal women with ankle fractures. *J Clin Endocrinol Metab.* 2011;96:2041–8.
33. Melton LJ 3rd, Riggs BL, Keaveny TM, et al. Relation of vertebral deformities to bone density, structure, and strength. *J Bone Miner Res.* 2010;25:1922–30.
34. Bjørnerem A, Bui QM, Ghasem-Zadeh A, Hopper JL, Zebaze R, Seeman E. Fracture risk and height: an association partly accounted for by cortical porosity of relatively thinner cortices. *J Bone Miner Res.* 2013;28:2017–26.
35. Stein EM, Liu XS, Nickolas TL, et al. Microarchitectural abnormalities are more severe in postmenopausal women with vertebral compared to nonvertebral fractures. *J Clin Endocrinol Metab.* 2012;97:E1918–26.
36. Roux JP, Wegrzyn J, Arlot ME, et al. Contribution of trabecular and cortical components to biomechanical behavior of human vertebrae: an ex vivo study. *J Bone Miner Res.* 2010;25:356–61.
37. Fields AJ, Eswaran SK, Jekir MG, Keaveny TM. Role of trabecular microarchitecture in whole-vertebral body biomechanical behavior. *J Bone Miner Res.* 2009;24:1523–30.
38. Stein EM, Liu XS, Nickolas TL, et al. Abnormal microarchitecture and reduced stiffness at the radius and tibia in postmenopausal women with fractures. *J Bone Miner Res.* 2010;25:2572–81.
39. Stein EM, Kepley A, Walker M, et al. Skeletal structure in postmenopausal women with osteopenia and fractures is characterized by abnormal trabecular plates and cortical thinning. *J Bone Miner Res.* 2014;29:1101–9.
40. Boutroy S, Khosla S, Sornay-Rendu E, et al. Microarchitecture and peripheral BMD are impaired in postmenopausal white women with fracture independently of total hip T-score: an international multicenter study. *J Bone Miner Res.* 2016;31:1158–66.
41. Nishiyama KK, Macdonald HM, Hanley DA, Boyd SK. Women with previous fragility fractures can be classified based on bone microarchitecture and finite element analysis measured with HR-pQCT. *Osteoporos Int.* 2013;24:1733–40.
42. Biver E, Durosier-Izart C, Chevalley T, van Rietbergen B, Rizzoli R, Ferrari S. Evaluation of radius microstructure and areal bone mineral density improves fracture prediction in postmenopausal women. *J Bone Miner Res.* 2018;33(2):328–37.
43. Szulc P, Debiecse E, Boutroy S, Vilauphiou N, Chapurlat R. Poor trabecular microarchitecture in male current smokers: the cross-sectional STRAMBO study. *Calcif Tissue Int.* 2011;89:303–11.
44. Rolland T, Boutroy S, Vilayphiou N, Blaizot S, Chapurlat R, Szulc P. Poor trabecular microarchitecture at the distal radius in older men with increased concentration of high-sensitivity C-reactive protein—the STRAMBO study. *Calcif Tissue Int.* 2012;90:496–506.
45. Argoud T, Boutroy S, Claustrat B, Chapurlat R, Szulc P. Association between sex steroid levels and bone microarchitecture in men: the STRAMBO study. *J Clin Endocrinol Metab.* 2014;99:1400–10.
46. Chaitou A, Boutroy S, Vilayphiou N, et al. Association of bone microarchitecture with parathyroid hormone concentration and calcium intake in men: the STRAMBO study. *Eur J Endocrinol.* 2011;165:151–9.
47. Bala Y, Bui QM, Wang XF, et al. Trabecular and cortical microstructure and fragility of the distal radius in women. *J Bone Miner Res.* 2015;30:621–9.
48. Bala Y, Zebaze R, Ghasem-Zadeh A, et al. Cortical porosity identifies women with osteopenia at increased risk for forearm fractures. *J Bone Miner Res.* 2014;29:1356–62.
49. Jing D, Cai J, Wu Y, et al. Pulsed electromagnetic fields partially preserve bone mass, microarchitecture, and strength by promoting bone formation in hindlimb-suspended rats. *J Bone Miner Res.* 2014;29:2250–61.
50. Vico L, van Rietbergen B, Vilayphiou N, et al. Cortical and trabecular bone microstructure did not recover at weight-bearing skeletal sites and progressively deteriorated at non-weight-bearing sites during the year following international space station missions. *J Bone Miner Res.* 2017;32:2010–21.
51. Riggs BL, Melton LJ 3rd, Robb RA, et al. Population-based study of age and sex differences in bone volumetric density, size, geometry, and structure at different skeletal sites. *J Bone Miner Res.* 2004;19:1945–54.
52. Macdonald HM, Nishiyama KK, Kang J, Hanley DA, Boyd SK. Age-related patterns of trabecular and cortical bone loss differ between sexes and skeletal sites: a population-based HR-pQCT study. *J Bone Miner Res.* 2011;26:50–62.